Nucleon spin-averaged forward virtual Compton tensor at large Q^{2}

Richard J. Hill and Gil Paz

Phys. Rev. D **95**, 094017 — Published 25 May 2017

DOI: 10.1103/PhysRevD.95.094017

FERMILAB-PUB-16-465-T
WSU-HEP-1607
November 29, 2016

Nucleon spin-averaged forward virtual Compton tensor at large Q^2

Richard J. Hill[a] and Gil Paz[b]

[a] *Perimeter Institute for Theoretical Physics, Waterloo, ON, N2L 2Y5 Canada, TRIUMF, 4004 Wesbrook Mall, Vancouver, BC, V6T 2A3 Canada, Fermi National Accelerator Laboratory, Batavia, Illinois 60510, USA, and The University of Chicago, Chicago, Illinois, 60637, USA*

[b] *Department of Physics and Astronomy Wayne State University, Detroit, Michigan 48201, USA*

Abstract

The nucleon spin-averaged forward virtual Compton tensor determines important physical quantities such as electromagnetically-induced mass differences of nucleons, and two-photon exchange contributions in hydrogen spectroscopy. It depends on two kinematic variables: ν, the virtual photon energy in the proton rest frame, and Q^2, the photon's invariant four-momentum squared. Using the operator product expansion, we calculate the tensor's large-Q^2 behavior for $\nu = 0$, including for the first time the full spin-2 contribution and correcting a previous result in the literature for the spin-0 contribution. Implications for the proton radius puzzle are discussed.

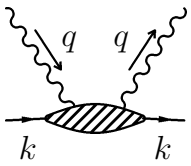

Figure 1: Forward scattering of virtual photon of momentum q^μ on hadron of momentum k^μ.

1 Introduction

The forward Compton amplitude describes virtual photon scattering on a hadron, depicted in Fig. 1, and encodes important structure information. For example, the spin-averaged proton forward Compton amplitude determines two-photon exchange (TPE) contributions to hydrogen spectroscopic transitions. These contributions dominate the uncertainty of the proton charge radius measured in muonic hydrogen [1] and have been the subject of recent intense scrutiny and controversy [2, 3, 4, 5]. The difference between spin-averaged proton and neutron forward Compton amplitudes determines the electromagnetic contribution to the proton-neutron mass splitting, also the subject of recent controversy [6, 7, 8, 9, 10].

The tensor representation of the spin-averaged Compton amplitude (cf. Eq. (1) below) involves two scalar functions, $W_1(\nu, Q^2)$ and $W_2(\nu, Q^2)$. The imaginary parts of these functions are determined by (elastic and inelastic) electron scattering data. $W_2(\nu, Q^2)$ can be reconstructed from its imaginary part using a dispersion relation in ν. However, $W_1(\nu, Q^2)$ requires a subtraction in the dispersion relation. Uncertainties related to the subtraction function for the proton, $W_1^p(0, Q^2)$, dominate the error budget for the muonic hydrogen Lamb shift. Similarly, uncertainties in the difference of subtraction functions for proton and neutron, $W_1^{p-n}(0, Q^2)$, dominate the error budget for the proton-neutron electromagnetic self energy. It is important to constrain this subtraction function.[1]

While not accessible directly from experimental data, we can constrain $W_1(0, Q^2)$ in the small- and large-Q^2 limits. For small Q^2 one can calculate [2] $W_1(0, Q^2)$ in terms of the Wilson coefficients of Non Relativistic QED (NRQED) [11, 12]. These coefficients are in turn determined by low-energy experimental measurements, or by nonperturbative QCD computations using lattice QCD or chiral perturbation theory. The Operator Product Expansion (OPE) may be used to show that $W_1(0, Q^2) \sim 1/Q^2$ for large Q^2 [7, 2]. In this paper we perform the explicit computation of the $1/Q^2$ coefficient in the OPE determination of $W_1(0, Q^2)$.

There are four types of operator that contribute to the coefficient of $1/Q^2$ in the OPE

[1] The need for subtraction is readily demonstrated: $W_1(\nu, 0) = -2 + \mathcal{O}(\nu^2)$ at low ν (see e.g. Ref. [12]), in contradiction with the prediction from an unsubtracted dispersion relation, $W_1(\nu, 0) = (1/\pi) \int_{\nu_{\rm cut}^2}^{\infty} d\nu'^2 {\rm Im} W_1(\nu', 0)/(\nu'^2 - \nu^2)$, which is manifestly positive using the optical theorem for ${\rm Im} W_1(\nu', 0)$ (see e.g. Ref. [2]). Reference [10] argues that after subtraction of a term motivated by Reggeon dominance, the remaining structure functions satisfy unsubtracted dispersion relations; however, a reliable evaluation of such a subtraction has not been presented.

expression for $W_1(0,Q^2)$: spin-0 quark, spin-0 gluon, spin-2 quark and spin-2 gluon. Previous analyses of $W_1(0,Q^2)$ are based on the work of Collins from 1979 [7], which was concerned with the renormalization of the Cottingham formula for electromagnetic mass splittings, and considered only the spin-0 operators. In this paper we calculate the Wilson coefficients for both types of operator. We correct an error in the expression for the spin-0 contribution in Ref. [7]. Applications to muonic hydrogen require inclusion of the spin-2 operators. Since these were not included before, existing applications are incomplete; in fact, we show that the spin-2 contribution is numerically dominant.

The remainder of the paper is structured as follows. In Sec. 2 we perform the analytic calculations of the Wilson coefficients. In particular we perform the one-loop calculations needed to extract the Wilson coefficients of gluon operators. In Sec. 3 we evaluate the relevant local nucleon matrix elements. Focusing on the proton case, we numerically evaluate $W_1(0,Q^2)$ at large Q^2. In Sec. 4 we discuss the implications of our results for TPE contributions to the muonic hydrogen Lamb shift. In Sec. 5 we present our conclusions.

2 Wilson coefficients

Here we introduce notation for the Compton amplitude and determine the relevant operators in the OPE. We then perform matching onto quark and gluon operators.

2.1 Preliminaries

The nucleon spin-averaged forward virtual Compton scattering tensor is defined as (cf. Fig. 1)

$$W_{\rm S}^{N\,\mu\nu}(\nu,Q^2) \equiv \frac{i}{2}\sum_s \int d^4x\, e^{iq\cdot x}\langle N(\boldsymbol{k},s)|T\{J^\mu_{\rm e.m.}(x)J^\nu_{\rm e.m.}(0)\}|N(\boldsymbol{k},s)\rangle\,, \tag{1}$$

where $\boldsymbol{k}$ is the nucleon three-momentum and s its spin, $J^\mu_{\rm e.m.}$ is the electromagnetic current, and the subscript S denotes symmetrization in μ and ν.[2] Here $N=p$ or $N=n$ denotes a proton or neutron. Also, $\nu = 2k\cdot q$ and $Q^2 = -q^2$. Notice that some authors refer to this quantity as $T^{\mu\nu}$ [7, 8].

Using current conservation, and invariance of electromagnetic interactions under parity and time-reversal, $W_{\rm S}^{N\,\mu\nu}$ can be expressed as

$$W_{\rm S}^{N\,\mu\nu} = \left(-g^{\mu\nu}+\frac{q^\mu q^\nu}{q^2}\right)W_1^N(\nu,Q^2) + \left(k^\mu - \frac{k\cdot q\, q^\mu}{q^2}\right)\left(k^\nu - \frac{k\cdot q\, q^\nu}{q^2}\right)W_2^N(\nu,Q^2)\,. \tag{2}$$

We will use relativistic normalization of states, $\bar{u}_N(k)u_N(k) = 2m_N$, for nucleon spinors throughout. The imaginary parts W_i^N are related to physical cross sections. Inserting a complete set of states into (1),

$$2\,{\rm Im}\,W_{\rm S}^{N\,\mu\nu} = \frac{1}{2}\sum_s \sum\!\!\!\!\!\!\int_X \Big[\langle N(\boldsymbol{k},s)|J^\mu|X\rangle\langle X|J^\nu|N(\boldsymbol{k},s)\rangle(2\pi)^4\delta^4(q-p_X+k)$$

[2] Symmetrization in μ and ν can be shown equivalent to spin averaging: if $W^{N\,\mu\nu}$ is expanded in a tensor basis, terms that are odd under $\mu\leftrightarrow\nu$ are linear in the nucleon spin vector, $S^\mu \propto \bar{u}_N(p,s)\gamma^\mu\gamma_5 u_N(p,s)$, and vanish under spin averaging; terms symmetric under $\mu\leftrightarrow\nu$ are independent of S^μ as displayed in Eq. (2).

$$+\langle N(\boldsymbol{k},s)|J^\nu|X\rangle\langle X|J^\mu|N(\boldsymbol{k},s)\rangle(2\pi)^4\delta^4(q+p_X-k)\Big]\,, \qquad (3)$$

where p_X is the momentum of the state X. We can now perform a separation between nucleon and non-nucleon (i.e., excited) states. The nucleon contributions to $\mathrm{Im}\,W_i^N$ can be expressed in terms of nucleon form factors. Contributions from other final states can be expressed in terms of inelastic structure functions. Using dispersion relations, W_2^N can be reconstructed from its imaginary part, but W_1^N requires a subtraction in order to have a convergent dispersion relation. Thus

$$W_1^N(\nu,Q^2) = W_1^N(0,Q^2) + \frac{\nu^2}{\pi}\int_0^\infty d\nu'^2\,\frac{\mathrm{Im}W_1^N(\nu',Q^2)}{\nu'^2(\nu'^2-\nu^2)}\,,$$

$$W_2^N(\nu,Q^2) = \frac{1}{\pi}\int_0^\infty d\nu'^2\,\frac{\mathrm{Im}W_2^N(\nu',Q^2)}{\nu'^2-\nu^2}\,. \qquad (4)$$

Since $W_1^N(0,Q^2)$ is not directly related to measured quantities it is a major source of uncertainty for quantities like the TPE contribution to the Lamb shift in muonic hydrogen [2] and the isovector nucleon electromagnetic self-energy [8]. As discussed in the introduction, we can constrain $W_1^N(0,Q^2)$ in the small-Q^2 and large-Q^2 limits. The small-Q^2 behavior was discussed in Ref. [2]. Here we will calculate the large Q^2 behavior.

We will determine the OPE for the operator,

$$T_{\rm S}^{\mu\nu}(q) \equiv i\int d^4x\, e^{iq\cdot x} T\{J^{\{\mu}_{\rm e.m.}(x) J^{\nu\}}_{\rm e.m.}(0)\}\,, \qquad (5)$$

where curly braces around indices denote symmetrization, i.e., $A^{\{\alpha}B^{\beta\}} = (A^\alpha B^\beta + B^\alpha A^\beta)/2$ for four-vectors A^μ and B^μ. Note that the Compton tensor is obtained by taking the matrix element, $W_{\rm S}^{N\,\mu\nu}(\nu,Q^2) = \langle N(\boldsymbol{k},s)|T_{\rm S}^{\mu\nu}|N(\boldsymbol{k},s)\rangle$. For the OPE evaluation we match onto the lowest dimension QCD operators, which begin at dimension four. There are four[3] relevant operator types

$$\begin{aligned}
O_f^{(0)} &= m_f \bar f f,\\
O_g^{(0)} &= G^A_{\alpha\beta}G^{A\alpha\beta},\\
O_f^{(2)\alpha\beta} &= \bar f\left(iD^{\{\alpha}\gamma^{\beta\}} - \frac{1}{d}\,i\not{D}g^{\alpha\beta}\right) f,\\
O_g^{(2)\alpha\beta} &= -G^{A\alpha\lambda}G^{A\beta}{}_\lambda + \frac{1}{d}g^{\alpha\beta}G^A_{\rho\sigma}G^{A\rho\sigma},
\end{aligned} \qquad (6)$$

where $d = 4-2\epsilon$ is the spacetime dimension, and $f = u, d, s, ...$ runs over active quark flavors. The superscript label denotes operator spin. The spin-2 operators are traceless, i.e. they satisfy $g_{\alpha\beta}O_{f,g}^{(2)\alpha\beta} = 0$.

[3] As we will see below, there is another possible structure $O_{\rm S}^{(r)\mu\alpha\nu\beta}$. The matrix element of the corresponding contribution to $T_S^{\mu\nu}$ between proton states vanishes, so we do not include it in Eq. (6). See Appendix A.

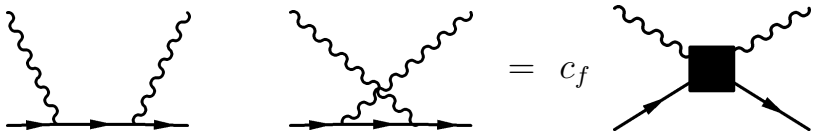

Figure 2: Quark matching condition. The right hand side denotes a sum over operators in Eq. (7).

Current conservation implies $q_\mu T^{\mu\nu} = q_\nu T^{\mu\nu} = 0$ up to operators whose physical matrix elements vanish. This implies that the general form[4] of $T_{\rm S}^{\mu\nu}$ may be written

$$\begin{aligned} T_{\rm S}^{\mu\nu} &= \frac{1}{q^2}\left(-g^{\mu\nu} + \frac{q^\mu q^\nu}{q^2}\right)\left(\sum_f c_{1f} O_f^{(0)} + c_{1g} O_g^{(0)}\right) \\ &+ \frac{1}{q^2}\left(-g^{\mu\nu} + \frac{q^\mu q^\nu}{q^2}\right)\frac{q_\alpha q_\beta}{q^2}\left(\sum_f c_{2f} O_f^{(2)\alpha\beta} + c_{2g} O_g^{(2)\alpha\beta}\right) \\ &+ \frac{1}{q^2}\left(-g_\alpha^\mu + \frac{q^\mu q_\alpha}{q^2}\right)\left(-g_\beta^\nu + \frac{q_\beta q^\nu}{q^2}\right)\left(\sum_f c_{3f} O_f^{(2)\alpha\beta} + c_{3g} O_g^{(2)\alpha\beta}\right) + \mathcal{O}\left(\frac{1}{q^4}\right). \end{aligned} \tag{7}$$

Using the matrix elements (20) and (25) below, we see that c_1 and c_2 will contribute to W_1 and c_3 to W_1 and W_2. Let us proceed to match onto quark and gluon operators at leading order in QCD perturbation theory.

2.2 Quark operators

In order to match onto the quark operators, we compute forward scattering amplitudes using on-shell quarks with electromagnetic charge e_f (in units of the proton charge), mass m_f, and four-momentum k as external states; cf. Fig. 2. The matrix element for $T_{\rm S}^{\mu\nu}$ between such states is

$$\langle f|T_{\rm S}^{\mu\nu}|f\rangle = -\sum_f \frac{2e_f^2}{q^2}\,\bar{u}_f(k)\left[k^\mu\gamma^\nu + k^\nu\gamma^\mu - \frac{2k\cdot q}{q^2}\left(q^\mu\gamma^\nu + q^\nu\gamma^\mu - g^{\mu\nu}\not{q}\right)\right]u_f(k) + \mathcal{O}\left(\frac{1}{q^4}\right). \tag{8}$$

After simplification this gives the results

$$2c_{1f} = c_{2f} = -c_{3f} = 4e_f^2\,. \tag{9}$$

The expression for c_{1f} agrees with equation 2.14 of Ref. [7]. The coefficients c_{2f} and c_{3f} were not considered in Ref. [7].

[4] A fourth possible term $q_\alpha q_\beta O_{\rm S}^{(r)\mu\alpha\nu\beta}$ is omitted since its matrix elements between spin-averaged proton states is zero.

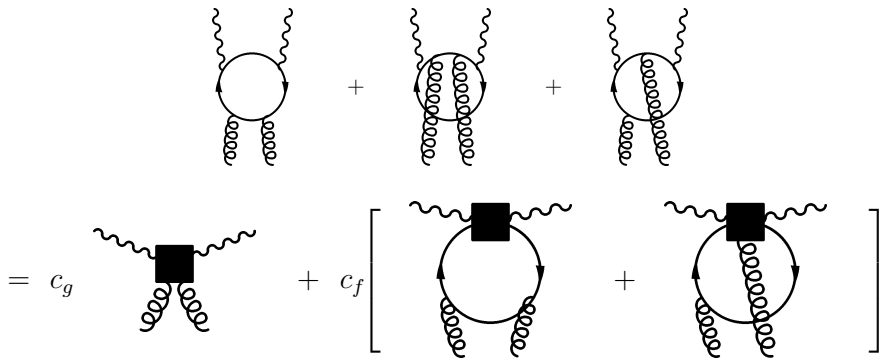

Figure 3: Matching condition onto gluon operators. The three diagrams on the left hand side denote the contributions $T_a^{\mu\nu}$, $T_b^{\mu\nu}$ and $T_c^{\mu\nu}$ in Eq. (10). The right hand side denotes a sum over operators in Eq. (7). Permutations of external states are not displayed.

2.3 Gluon operators

The calculation of c_{ig} is simplified by using a background field analysis in Fock-Schwinger gauge [13]. We then have the following expressions for the gluon contributions to $T^{\mu\nu}$,

$$
\begin{aligned}
T_a^{\mu\nu} &= -\frac{ig^2}{4}\mathrm{Tr}\left[t^a t^b\right] G^a_{\rho\alpha}(0) G^b_{\sigma\beta}(0) \sum_f e_f^2 \int \frac{d^dl}{(2\pi)^d} \frac{\partial}{\partial k_\rho} \frac{\partial}{\partial k'_\sigma} \\
&\quad \mathrm{Tr}\left[\gamma^\mu \frac{1}{\not l - m_f} \gamma^\alpha \frac{1}{\not l - \not k - m_f} \gamma^\beta \frac{1}{\not l - \not k - \not k' - m_f} \gamma^\nu \frac{1}{\not l - \not q - m_f}\right]_{k=k'=0}, \\
T_b^{\mu\nu} &= -\frac{ig^2}{4}\mathrm{Tr}\left[t^a t^b\right] G^a_{\rho\alpha}(0) G^b_{\sigma\beta}(0) \sum_f e_f^2 \int \frac{d^dl}{(2\pi)^d} \frac{\partial}{\partial k_\rho} \frac{\partial}{\partial k'_\sigma} \\
&\quad \mathrm{Tr}\left[\gamma^\mu \frac{1}{\not l - m_f} \gamma^\nu \frac{1}{\not l - \not q + \not k + \not k' - m_f} \gamma^\alpha \frac{1}{\not l - \not q + \not k' - m_f} \gamma^\beta \frac{1}{\not l - \not q - m_f}\right]_{k=k'=0}, \\
T_c^{\mu\nu} &= -\frac{ig^2}{4}\mathrm{Tr}\left[t^a t^b\right] G^a_{\rho\alpha}(0) G^b_{\sigma\beta}(0) \sum_f e_f^2 \int \frac{d^dl}{(2\pi)^d} \frac{\partial}{\partial k_\rho} \frac{\partial}{\partial k'_\sigma} \\
&\quad \mathrm{Tr}\left[\gamma^\mu \frac{1}{\not l - m_f} \gamma^\alpha \frac{1}{\not l - \not k - m_f} \gamma^\nu \frac{1}{\not l - \not q + \not k' - m_f} \gamma^\beta \frac{1}{\not l - \not q - m_f}\right]_{k=k'=0},
\end{aligned}
\tag{10}
$$

where we separate $T^{\mu\nu}$ into three pieces, $T_a^{\mu\nu}$, $T_b^{\mu\nu}$, and $T_c^{\mu\nu}$, as illustrated in Fig. 3. The contributions $T_a^{\mu\nu}$ and $T_b^{\mu\nu}$ are equal and IR divergent, while $T_c^{\mu\nu}$ is IR finite. In the following we will work in $d = 4 - 2\epsilon$ dimensions to regularize these IR divergences and set the quark masses to zero. The effective theory loop diagrams pictured in Fig. 3 then vanish. We note also that none of $T_a^{\mu\nu}$, $T_b^{\mu\nu}$ or $T_c^{\mu\nu}$ obeys current conservation by itself, only their sum.

Since $T_c^{\mu\nu}$ is IR finite we can set $d = 4$ and get

$$T_c^{\mu\nu} = \sum_f e_f^2 \frac{g^2}{16\pi^2}\frac{1}{q^2}\left[\frac{1}{3}O_g^{(0)}\left(-g^{\mu\nu}+\frac{q^\mu q^\nu}{q^2}\right)+2\frac{q^\mu q_\alpha}{q^2}O_g^{(2)\alpha\nu}+2\frac{q^\nu q_\alpha}{q^2}O_g^{(2)\alpha\mu}-4\frac{q_\alpha q_\beta}{q^2}O_{\rm S}^{(r)\mu\alpha\nu\beta}\right], \tag{11}$$

where $q_\alpha q_\beta O_{\rm S}^{(r)\mu\alpha\nu\beta}$ is an operator structure whose nucleon matrix element vanishes, cf. Appendix A. $T_a^{\mu\nu}$ is IR divergent and we calculate it in $d = 4-2\epsilon$ dimensions. We find

$$\begin{aligned} T_a^{\mu\nu} = T_b^{\mu\nu} = \sum_f e_f^2 \frac{g^2}{24\pi^2}\frac{1}{q^2}\left(\frac{4\pi\mu^2}{-q^2-i0}\right)^\epsilon \Gamma(2+\epsilon)\mathrm{B}(2-\epsilon,1-\epsilon)\times \\ \times\left[\frac{q^\mu q^\nu q_\alpha q_\beta}{q^4}O_g^{(2)\alpha\beta}(-4-2\epsilon)+\frac{q_\alpha q_\beta g^{\mu\nu}}{q^2}O_g^{(2)\alpha\beta}\left(\frac{4-5\epsilon+2\epsilon^2}{\epsilon}\right)\right. \\ \left.+\left(\frac{q_\alpha q^\mu}{q^2}O_g^{(2)\alpha\nu}+\frac{q_\alpha q^\nu}{q^2}O_g^{(2)\alpha\mu}\right)\left(\frac{-4+6\epsilon}{\epsilon}\right)+O_g^{(2)\mu\nu}\left(\frac{4-5\epsilon}{\epsilon\,(1+\epsilon)}\right)\right]. \end{aligned} \tag{12}$$

Expanding in ϵ and adding $T_a^{\mu\nu}, T_b^{\mu\nu}$, and $T_c^{\mu\nu}$, we have the total gluon contribution

$$\begin{aligned} T_{\rm gluon}^{\mu\nu} = \sum_f e_f^2 \frac{\alpha_s}{4\pi}\frac{1}{q^2}\left[\frac{1}{3}\left(-g^{\mu\nu}+\frac{q^\mu q^\nu}{q^2}\right)O_g^{(0)}-4\frac{q_\alpha q_\beta}{q^2}O_{\rm S}^{(r)\mu\alpha\nu\beta}\right. \\ +\left(-\frac{8}{3\epsilon}-\frac{14}{3}-\frac{8}{3}\log\frac{\mu^2}{-q^2}\right)\left(-g^{\mu\nu}+\frac{q^\mu q^\nu}{q^2}\right)\frac{q_\alpha q_\beta}{q^2}O_g^{(2)\alpha\beta} \\ \left.+\left(\frac{8}{3\epsilon}+2+\frac{8}{3}\log\frac{\mu^2}{-q^2}\right)\left(-g_\alpha^\mu+\frac{q^\mu q_\alpha}{q^2}\right)\left(-g_\beta^\nu+\frac{q_\beta q^\nu}{q^2}\right)O_g^{(2)\alpha\beta}\right], \end{aligned} \tag{13}$$

from which we may read off the coefficients c_{ig}. Here we have introduced the renormalized strong coupling in the $\overline{\rm MS}$ scheme,

$$g_{\rm bare}^2\mu^{-2\epsilon}(4\pi)^\epsilon\Gamma(1+\epsilon) = \alpha_s + \mathcal{O}(\alpha_s^2)\,. \tag{14}$$

As an alternative approach, inspection of Eq. (7) shows that the coefficients c_1, c_2 and c_3 may be extracted from the quantity $v_\mu v_\nu T^{\mu\nu}$, for arbitrary timelike unit vector v^μ ($v^2 = 1$):

$$\begin{aligned} v_\mu v_\nu T_{\rm gluon}^{\mu\nu} = c_{1g}\frac{1}{q^2}\left(-1+\frac{(v\cdot q)^2}{q^2}\right)O_g^{(0)}+\frac{q_\alpha q_\beta}{q^4}O_g^{(2)\alpha\beta}\left[\left(-1+\frac{(v\cdot q)^2}{q^2}\right)c_{2g}+\frac{(v\cdot q)^2}{q^2}c_{3g}\right] \\ +c_{3g}\left(\frac{v_\alpha v_\beta}{q^2}-2\frac{v\cdot q q_\alpha v_\beta}{q^4}\right)O_g^{(2)\alpha\beta}\,. \end{aligned} \tag{15}$$

Following the notation of Ref. [14], we write[5]

$$v_\mu v_\nu T_k^{\mu\nu} = -\frac{ig^2}{8}\left[\frac{1}{d(d-1)}O_g^{(0)}I_k^{(0)}(q)+\frac{1}{d-2}O_g^{(2)\alpha\beta}I_{k\,\alpha\beta}^{(2)}(q)\right]. \tag{16}$$

[5]For our case, we need the "ZZ" contribution from Ref. [14], with axial coefficient $c_A = 0$ and vector coefficient $c_V = e_f$.

Neglecting quark masses, we have[6]

$$
\begin{aligned}
I_a^{(0)}(q) &= 0\,, \\
I_c^{(0)}(q) &= [c_\epsilon]\frac{\sum_f e_f^2}{-q^2}\left[32 - 32\frac{(v\cdot q)^2}{q^2}\right], \\
I_{a\,\mu\nu}^{(2)}(q) &= [c_\epsilon]\frac{\sum_f e_f^2}{(-q^2)^{1+\epsilon}}\left[v_\mu v_\nu\left(-\frac{64}{3\epsilon}+\frac{16}{3}\right) + \frac{v\cdot q v_\mu q_\nu}{q^2}\left(\frac{128}{3\epsilon}+\frac{64}{3}\right) + \frac{q_\mu q_\nu}{q^2}\left(-\frac{64}{3\epsilon}-16\right)\right. \\
&\qquad \left. + \frac{q_\mu q_\nu (v\cdot q)^2}{q^4}\left(\frac{64}{3}\right) + \mathcal{O}(\epsilon)\right], \\
I_{c\,\mu\nu}^{(2)}(q) &= [c_\epsilon]\frac{\sum_f e_f^2}{(-q^2)^{1+\epsilon}}\left[-64\frac{v\cdot q v_\mu q_\nu}{q^2} + \mathcal{O}(\epsilon)\right],
\end{aligned}
\tag{17}
$$

with $[c_\epsilon] \equiv i\Gamma(1+\epsilon)(4\pi)^{-2+\epsilon}$. Thus, either from Eq. (13) or from Eqs. (15) and (16), we read off the bare matching coefficients,

$$
\begin{aligned}
c_{1g}^{\rm bare} &= \frac{\alpha_s}{4\pi}\sum_f e_f^2\left(\frac{1}{3}\right), \\
c_{2g}^{\rm bare} &= \frac{\alpha_s}{4\pi}\sum_f e_f^2\left(\frac{-q^2}{\mu^2}\right)^{-\epsilon}\left(-\frac{8}{3\epsilon}-\frac{14}{3}\right), \\
c_{3g}^{\rm bare} &= \frac{\alpha_s}{4\pi}\sum_f e_f^2\left(\frac{-q^2}{\mu^2}\right)^{-\epsilon}\left(\frac{8}{3\epsilon}+2\right).
\end{aligned}
\tag{18}
$$

Renormalizing operators in the $\overline{\rm MS}$ scheme [14], we find the renormalized coefficients,

$$
\begin{aligned}
c_{1g}(\mu) &= \frac{\alpha_s}{4\pi}\sum_f e_f^2\left(\frac{1}{3}\right), \\
c_{2g}(\mu) &= \frac{\alpha_s}{4\pi}\sum_f e_f^2\left(-\frac{14}{3}+\frac{8}{3}\log\frac{Q^2}{\mu^2}\right), \\
c_{3g}(\mu) &= \frac{\alpha_s}{4\pi}\sum_f e_f^2\left(2-\frac{8}{3}\log\frac{Q^2}{\mu^2}\right).
\end{aligned}
\tag{19}
$$

3 Nucleon matrix elements

Here we evaluate the relevant nucleon matrix elements. In Secs. 3.1 and 3.2, we discuss the spin-0 and spin-2 matrix elements for both proton and neutron. In Sec. 3.3 we specialize to

[6] A non-propagating typo appears in Eq. (83) of Ref. [14]: in $N_{a\,\mu\nu(ZZ)}^{(2)}$, in the $z_2 L_\mu L_\nu$ term, the opposite sign should appear in front of $x(2-x-\epsilon)$.

the proton case and provide explicit numerical results for the leading $1/Q^2$ OPE evaluation of $W_1^p(0,Q^2)$.

3.1 Spin zero

Following Ref. [15] let us define[7]

$$\langle N(k)|O_f^{(0)}|N(k)\rangle \equiv 2m_N^2 f_{f,N}^{(0)}\,, \quad \langle N(k)|O_g^{(0)}(\mu)|N(k)\rangle \equiv -2m_N^2 \tilde{f}_{g,N}^{(0)}(\mu)\,, \tag{20}$$

where we are using relativistic normalization $\bar{u}(k)u(k) = 2m_N$ for nucleon spinors.[8] The gluon matrix element is determined by the mass sum rule,

$$1 = (1-\gamma_m)\sum_f f_{q,N}^{(0)} - \frac{\tilde{\beta}}{2}\tilde{f}_{g,N}^{(0)}\,. \tag{21}$$

Here $\tilde{\beta}$ and γ_m denote the QCD beta function and mass anomalous dimension, whose leading expansions are

$$\begin{aligned}\tilde{\beta} &= \frac{\beta}{g} = -\sum_{k=1}\beta_{k-1}\left(\frac{\alpha_s}{4\pi}\right)^k\,, \quad \beta_0 = 11 - \frac{2}{3}n_f\,,\\ \gamma_m &= -\sum_{k=1}\gamma_{k-1}\left(\frac{\alpha_s}{4\pi}\right)^k\,, \quad \gamma_0 = 8\,,\end{aligned} \tag{22}$$

where n_f is the number of active quark flavors.[9] For the quark matrix elements we use

$$2m_N\Sigma_{\pi N} = \frac{m_u+m_d}{2}\langle N|(\bar{u}u+\bar{d}d)|N\rangle\,, \quad 2m_N\Sigma_- = (m_d-m_u)\langle N|(\bar{u}u-\bar{d}d)|N\rangle\,. \tag{23}$$

In terms of the quark mass ratio $R_{ud}\equiv m_u/m_d$ we have

$$f_{u,N}^{(0)} = \frac{R_{ud}}{1+R_{ud}}\frac{\Sigma_{\pi N}}{m_N}(1+\xi)\,, \quad f_{d,N}^{(0)} = \frac{1}{1+R_{ud}}\frac{\Sigma_{\pi N}}{m_N}(1-\xi)\,, \quad \xi = \frac{1+R_{ud}}{1-R_{ud}}\frac{\Sigma_-}{2\Sigma_{\pi N}}\,. \tag{24}$$

Numerical values for spin-zero matrix elements are summarized in Table 1. As detailed in Ref. [15], the matrix elements $f_{u,d,s}^{(0)}$ are identical for $n_f = 3$ and $n_f = 4$, up to power corrections.

3.2 Spin two

Let us define

$$\langle N(k)|O_f^{(2)\mu\nu}(\mu)|N(k)\rangle \equiv 2\left(k^\mu k^\nu - \frac{g^{\mu\nu}}{4}m_N^2\right)f_{f,N}^{(2)}(\mu)\,,$$

[7]Compared to the quantity $f_{g,N}^{(0)}$ in Ref. [15], we have $\tilde{f}_{g,N}^{(0)} = [8\pi/(9\alpha_s)]f_{g,N}^{(0)}$. The conventional 8/9 prefactor is designed to simplify the expression for the sum rule (21) when $n_f = 3$.

[8]Recall that the nonrelativistic normalization $\bar{u}(k)u(k) = m_N/E_{\boldsymbol{k}}$ was used in Ref. [15].

[9]Higher order terms are listed in Ref. [15]. In numerical applications of Eq. (21), we evaluate γ_m and $\tilde{\beta}$ through $\mathcal{O}(\alpha_s^4)$.

quantity	value	reference
$\Sigma_{\pi N}$	44(13) MeV	[16, 17, 18, 19, 20, 21]
Σ_-	$\pm$2(2) MeV	[22, 23]
R_{ud}	0.48(10)	[24]
$m_N f_{s,N}^{(0)}$	40(20) MeV	[25]
$m_N f_{c,N}^{(0)}$ (lattice)	80(30) MeV	[26, 27, 19]
$m_N f_{c,N}^{(0)}$ (pQCD)	69(3) MeV	[15]

Table 1: Spin-zero operator matrix elements. For $\Sigma_{\pi N}$, the value is taken from Ref. [16] as in Ref. [15], and encompasses more recent results of Refs. [17, 18, 19, 20, 21]. The upper (lower) sign in Σ_- is for the proton (neutron). The neutron form factors follow from approximate isospin symmetry expressed in (27). For $f_{s,N}^{(0)}$ we assume a conservative 50% uncertainty compared to the estimate of 25% in Ref. [25]. For $f_{c,N}^{(0)}$ the value 80(30) MeV encompasses the results of Refs. [26, 27, 19].

quantity	value
$f_{u,p}^{(2)}(\mu = 2\,\text{GeV})$	0.346(6)
$f_{d,p}^{(2)}(\mu = 2\,\text{GeV})$	0.192(5)
$f_{s,p}^{(2)}(\mu = 2\,\text{GeV})$	0.034(2)
$f_{c,p}^{(2)}(\mu = 2\,\text{GeV})$	0.0088(3)

Table 2: Spin-two proton matrix elements derived from MSTW analysis [28] with $n_f = 4$ at $\mu = 2\,\text{GeV}$. The neutron form factors follow from approximate isospin symmetry expressed in Eq. (27).

$$\langle N(k)|O_g^{(2)\mu\nu}(\mu)|N(k)\rangle \equiv 2\left(k^\mu k^\nu - \frac{g^{\mu\nu}}{4}m_N^2\right) f_{g,N}^{(2)}(\mu)\,. \tag{25}$$

The gluon matrix element is determined by the momentum sum rule,

$$\sum_f f_{f,N}^{(2)}(\mu) + f_{g,N}^{(2)}(\mu) = 1\,. \tag{26}$$

Up to corrections proportional to $m_u - m_d$ and α, the proton and neutron matrix elements are related as,

$$\langle p|O_u^{(2)}|p\rangle = \langle n|O_d^{(2)}|n\rangle\,, \quad \langle p|O_d^{(2)}|p\rangle = \langle n|O_u^{(2)}|n\rangle\,, \quad \langle p|O_s^{(2)}|p\rangle = \langle n|O_s^{(2)}|n\rangle\,. \tag{27}$$

For the numerical evaluation, we use the inputs of Table 2 for $n_f = 4$ at $\mu = 2\,\text{GeV}$, with gluon matrix element given by Eq. (26). For different μ in the limited range considered, we employ the leading log renormalization (cf. Table 5 of Ref. [15]).

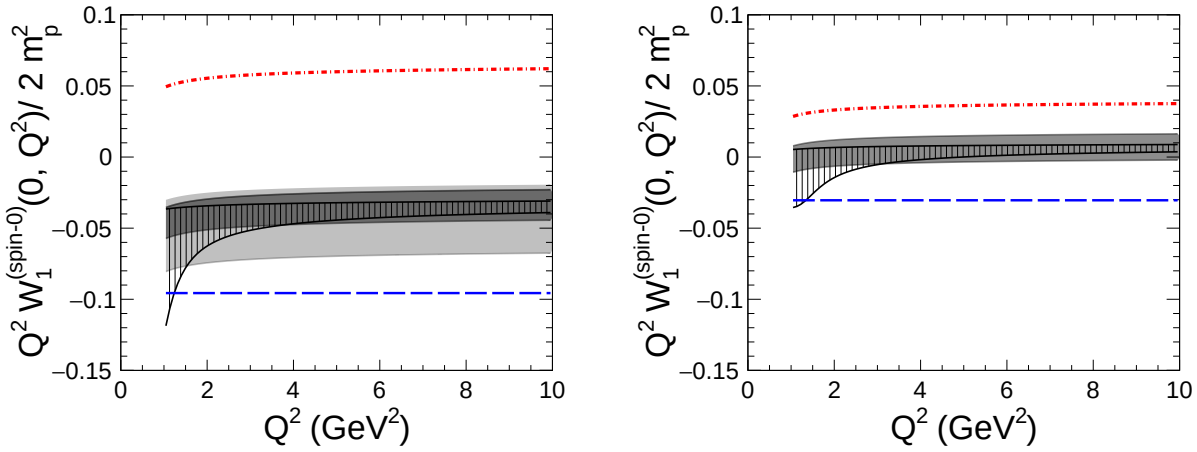

Figure 4: Spin-0 contribution to $Q^2\,W_1(0,Q^2)/2m_p^2$ as a function of Q^2. The final results are given with $n_f = 4$ in the left-hand plot. For comparison, results with $n_f = 3$ are in the right-hand plot. The black band with vertical stripes displays the result with perturbative uncertainty estimated by renormalization scale variation $Q/2 < \mu < 2Q$. The solid bands represent hadronic uncertainty from local matrix elements in Table 1. In the $n_f = 4$ evaluation, dark and light solid bands are obtained using $f_c^{(0)}$(pQCD) and $f_c^{(0)}$(lattice), respectively. The bottom dashed blue line and top dash-dotted red line give the separate quark and gluon contributions to the central value.

3.3 Large Q^2 behavior of $W_1(0,Q^2)$: numerical results

Let us restrict attention to the subtraction function for the proton, $W_1^p(0,Q^2)$. For notational simplicity we suppress the superscript, $W_1^p \to W_1$, in the following. In terms of the matrix elements of the previous section, we have the leading power result

$$W_1(0,Q^2) = \frac{2m_p^2}{Q^2}\left\{ -\sum_f c_{1f} f_f^{(0)} + c_{1g}\tilde{f}_g^{(0)} + \frac{1}{4}\left[\sum_f (c_{2f} - c_{3f})\, f_f^{(2)} + (c_{2g} - c_{3g})\, f_g^{(2)}\right]\right\}, \quad (28)$$

where the first nonvanishing order for coefficients of each operator are given by Eqs. (9) and (19). Let us consider separately the spin-0 and spin-2 contributions.

3.3.1 Spin-0: numerical evaluation for proton

Substituting the Wilson coefficients from Eqs. (9) and (19), the spin-0 contribution is

$$\frac{Q^2}{2m_p^2} W_1^{(\text{spin}-0)}(0,Q^2) = -2\sum_f e_f^2 f_f^{(0)} + \left(\sum_f e_f^2\right)\frac{\alpha_s}{12\pi}\tilde{f}_g^{(0)}(\mu)\,. \quad (29)$$

This contribution is displayed in Fig. 4 using $n_f = 4$ and $n_f = 3$. Having neglected quark masses, our $n_f = 4$ result is formally valid in the $m_c^2 \ll Q^2$ regime. Alternatively, an evaluation

using $n_f = 3$ is formally valid in the regime $\Lambda^2_{\rm QCD} \ll Q^2 \ll m_c^2$. We show below that $W_1(0,Q^2)$ is numerically dominated by the spin-2 contribution, and do not pursue a more elaborate analysis of charm quark mass dependence in the spin-0 contribution.

We take $n_f = 4$ in our final result. Fig. 4 compares results using different values of the charm scalar matrix element, $f_c^{(0)}$. As default, we use the perturbative QCD value obtained from expanding in $\Lambda_{\rm QCD}/m_c$ [15]. For comparison, Fig. 4 displays the range of $f_c^{(0)}$ from currently available $n_f = 4$ lattice QCD evaluations [26, 27, 19]. The gluon matrix element is given by Eq. (21), with $\tilde{\beta}$ and γ_m evaluated through $\mathcal{O}(\alpha_s^4)$. We choose default renormalization scale $\mu = Q$, and perturbative scale uncertainty is estimated by varying $Q/2 < \mu < 2Q$. We remark that a partial cancellation occurs between quark and gluon matrix elements, as illustrated in the figure.

The spin-0 part disagrees with Collins's calculation [7]. Equation 2.18 of Ref. [7] is

$$W_1^{(\text{spin}-0)}(0,Q^2)^{\rm Collins} = \frac{1}{Q^2}\left\{\frac{4KM^2}{a} - \sum_i \left(\frac{2K}{a} + 2\kappa_i^2\right)\langle p|m_{iB}\bar{\psi}_i\psi_i|p\rangle\right\}, \tag{30}$$

where $M = m_p$ is the proton mass, $K/a = n_f/(3\beta_0)$ with β_0 given by Eq. (22), κ_i is the quark charge (which we have denoted e_i), and m_{Bi} is the bare quark mass. In our notation,

$$W_1^{(\text{spin}-0)}(0,Q^2)^{\rm Collins} = \frac{2m_p^2}{Q^2}\left\{\frac{2n_f}{3\beta_0} - \sum_i \left(\frac{2n_f}{3\beta_0} + 2e_i^2\right) f_i^{(0)}\right\}. \tag{31}$$

Comparing with our result for the spin-0 part (29), and using the relation (21) with $\gamma_m = 0$ and $\tilde{\beta} = -\alpha_s\beta_0/(4\pi)$, we see that the replacement $n_f \to \sum_{f=u,d,s} e_f^2$ must be made in Collins's expression (31) to obtain the correct result.

3.3.2 Spin-2: numerical evaluation for proton

Substituting the Wilson coefficients from Eqs. (9) and (19), the spin-2 contribution is

$$\frac{Q^2}{2m_p^2}W_1^{(\text{spin}-2)}(0,Q^2) = 2\sum_f e_f^2 f_f^{(2)} + \left(\sum_f e_f^2\right)\frac{\alpha_s}{4\pi}\left(-\frac{5}{3} + \frac{4}{3}\log\frac{Q^2}{\mu^2}\right) f_g^{(2)}(\mu), \tag{32}$$

where we retain the first non-vanishing contribution to each operator matching coefficient. This result is displayed in Fig. 4. For definiteness, we employ the $n_f = 4$ results from Table 2, although the contributions from strange and charm quark are negligible. The result is dominated by the up quark, with small contributions from down quark and gluon; the latter contributes a sizable fraction of the uncertainty as indicated in the figure.

3.3.3 Total

The complete OPE evaluation of $W_1(0,Q^2)$ for the proton is given by the sum of spin-0 and spin-2 contributions, and is displayed in Fig. 6. The result is dominated by the spin-2 contribution.

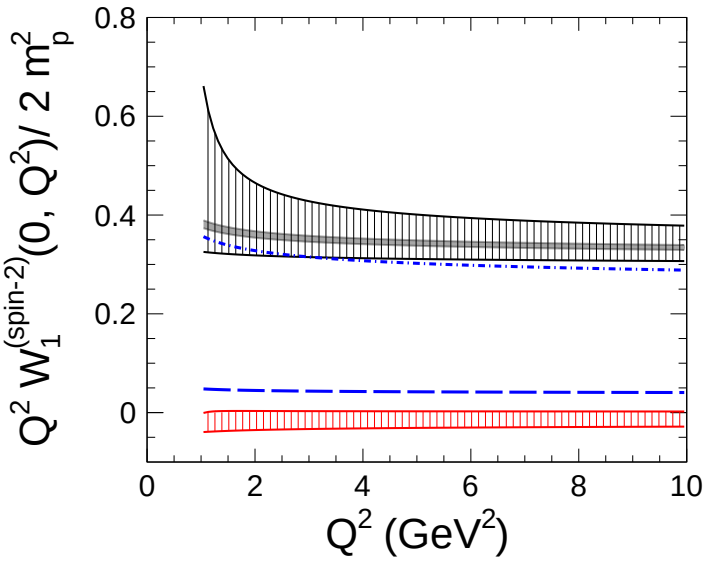

Figure 5: Spin-2 contribution to $Q^2\, W_1(0, Q^2)/2m_p^2$ as a function of Q^2. The dark gray band represents hadronic uncertainty. The vertically hatched band represents perturbative uncertainty, estimated by varying renormalization scale $Q/2 < \mu < 2Q$. Upper dash-dotted and lower dashed blue lines represent the contributions of up-quark and down-quark to the central value, and the lower red hatched band shows the gluon contribution and uncertainty.

4 Two photon exchange in muonic hydrogen Lamb shift

As detailed in Ref. [2], the piece of the TPE contribution to the muonic hydrogen Lamb shift that is not fully determined by electron scattering data involves the subtraction function in the dispersion relation for the forward Compton amplitude of the proton, i.e. $W_1(0, Q^2)$. Having constrained this function at both high- and low-Q^2, let us consider the implications for muonic hydrogen. Here we construct an interpolation of this function with the correct coefficients of $(Q^2)^0$ and $(Q^2)^1$ at low Q^2, the correct coefficient of $1/Q^2$ at high Q^2, and higher order terms parameterized by Λ_L and Λ_H introduced below.

Recall that at low-Q^2, we have the expansion, [2]

$$W_1(0, Q^2)_L = 2a_p(2 + a_p) + \frac{Q^2}{m_p^2}\left\{ \frac{2m_p^3\bar{\beta}}{\alpha} - a_p - \frac{2}{3}\left[(1 + a_p)^2 m_p^2 (r_M^p)^2 - m_p^2 (r_E^p)^2\right]\right\}\left[1 + \Delta_L(Q^2)\right], \quad (33)$$

where the anomalous magnetic moment of the proton is $a_p = 1.793$, the magnetic polarizability of the proton[10] is $\bar{\beta} = 2.5(4) \times 10^{-4}\,\mathrm{fm}^3$ [24], and the proton magnetic and electric radii are

[10] See e.g. Ref. [12] for the definition of $\bar{\beta}$, which is there denoted β_M.

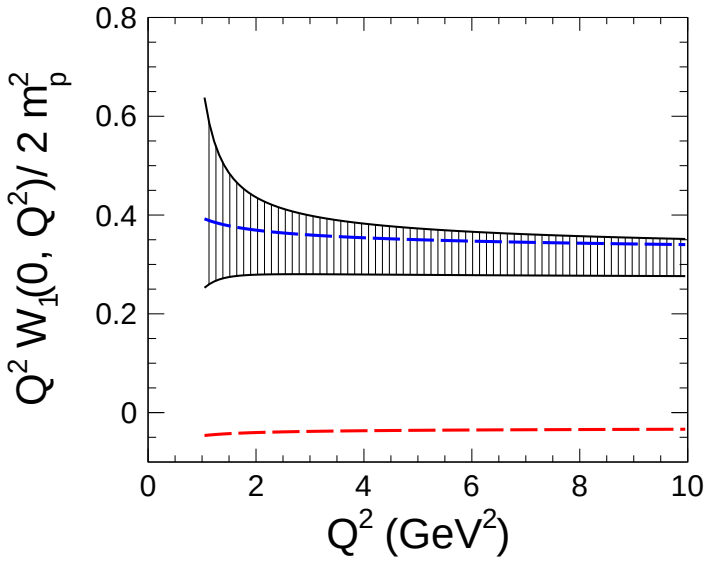

Figure 6: Total $Q^2\, W_1(0, Q^2)/2m_p^2$ as a function of Q^2. The dashed red and blue lines denote central values for the spin-0 and spin-2 contributions. The vertical hatched black band is the total contribution, with perturbative and hadronic errors from each of the spin-0 and spin-2 contributions added in quadrature.

$r_M = 0.776(34)(17)\,\text{fm}$ [29, 24], $r_E = 0.8751(61)\,\text{fm}$ [30, 24].[11] Here $\Delta_L(Q^2)$ accounts for terms of order Q^4 and higher in the Taylor expansion. To investigate sensitivity to these terms we consider

$$\Delta_L(Q^2) = \pm \frac{Q^2}{\Lambda_L^2}\,, \tag{34}$$

with hadronic scale $\Lambda_L \approx 500\,\text{MeV}$.

For the high-Q^2 behavior we have

$$W_1(0, Q^2)_H = \frac{2m_p^2}{Q^2} A(Q^2) \left[1 + \Delta_H(Q^2)\right], \tag{35}$$

where $A(Q^2)$ is the leading power result displayed in Fig. 6, and $\Delta(Q^2)$ accounts for power corrections (including charm mass corrections). To investigate the impact of power-suppressed terms we take central value $\Delta_H = 0$, and upper and lower envelopes

$$\Delta_H(Q^2) = \pm \frac{\Lambda_H^2}{Q^2}\,, \tag{36}$$

with hadronic scale $\Lambda_H \approx 500\,\text{MeV}$. Fig. 7 displays a cubic spline interpolation of $W_1(0, Q^2)$ taking the low-Q^2 and high-Q^2 inputs from NRQED and OPE. We show results for central

[11] After accounting for other uncertainties, the results of the interpolation for $\delta E(2S)^{W_1(0,Q^2)}$ are not significantly altered by using the muonic hydrogen value, $r_E = 0.84087(26)(29)\,\text{fm}$ [31, 24].

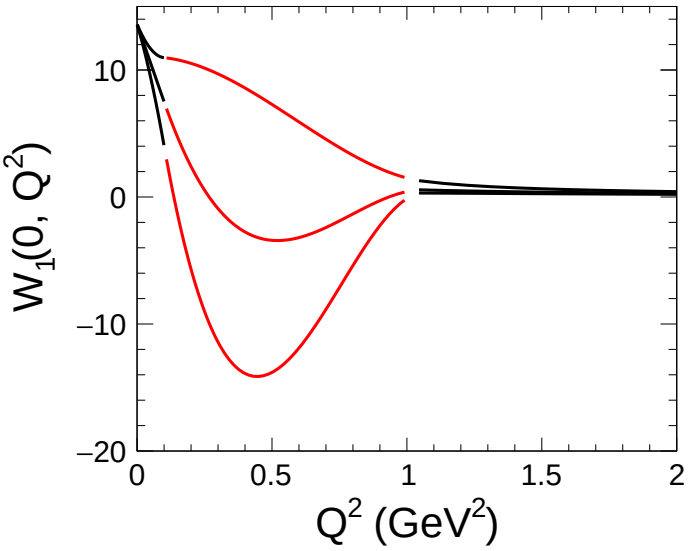

Figure 7: $W_1(0,Q^2)$ as a function of Q^2. Solid black curves on the left and right are from Eqs. (33) and (35), as explained in the text. Intermediate red curves are interpolations from the central curves and envelopes.

values, and for the interpolations based on upper and lower envelopes for the low-Q^2 ($Q^2 < Q_L^2$) and high-Q^2 ($Q^2 > Q_H^2$) constraints. For our default illustration we take $Q_L^2 = 0.1\,\mathrm{GeV}^2$ and $Q_H^2 = 1\,\mathrm{GeV}^2$. At low-$Q^2$ these envelopes account for uncertainties in low-energy constants appearing in Eq. (33), and for curvature and higher order corrections according to Eq. (34).[12] At high-Q^2 these envelopes account for perturbative and hadronic matrix element uncertainties in $A(Q^2)$ from Fig. 6, and for power corrections according to Eq. (36).[13] The intermediate region is outside of the domain of validity of either NRQED at low-Q^2, or OPE at high-Q^2.

The relevant TPE contribution to muonic hydrogen may be written

$$\delta E(\mathrm{2S})^{W_1(0,Q^2)} = \frac{\alpha^2}{m_\mu m_p}|\psi_{2\mathrm{S}}(0)|^2 \int_0^\infty dQ\, k(Q)\big[W_1(0,Q^2) - \lim_{Q^2\to 0} W_1(0,Q^2)\big]\,, \tag{37}$$

where $|\psi_{2S}(0)|^2 = m_r^3\alpha^3/(8\pi)$ for the 2S atomic state, and $k(Q)$ is the kinematic function

$$k(Q) = \frac{4}{\pi}\frac{m_\mu^2}{Q}\int_{-1}^1 dx\,\frac{\sqrt{1-x^2}(1+2x^2)}{Q^2+4m_\mu^2x^2}\,. \tag{38}$$

After subtracting the $Q^2 = 0$ limit, and rescaling with $k(Q)$, the interpolated function is displayed in the LHS of Fig. 8. The energy shift in Eq. (37) is proportional to the area under the curve in Fig. 8. For the central curve we obtain $\delta E(\mathrm{2S})^{W_1(0,Q^2)} = -0.034\,\mathrm{meV}$, and for the interpolated envelopes displayed in the figure, we find the interval

$$\delta E(\mathrm{2S})^{W_1(0,Q^2)}\big|_{\text{Fig. 8}} \in [-0.046\,\mathrm{meV},\ -0.021\,\mathrm{meV}]\,. \tag{39}$$

[12] Choosing a lower cutoff $Q_L^2 = 0.05\,\mathrm{GeV}^2$ would give $[-0.043\,\mathrm{meV}, -0.023\,\mathrm{meV}]$ in place of Eq. (39).
[13] Choosing a higher cutoff $Q_H^2 = 2\,\mathrm{GeV}^2$ would give $[-0.052\,\mathrm{meV},\ -0.020\,\mathrm{meV}]$ in place of Eq. (39).

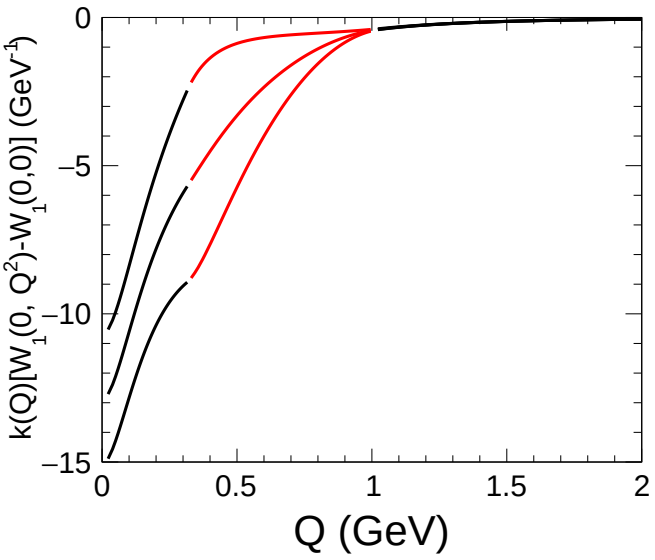

Figure 8: $W_1(0,Q^2)$, after subtracting $Q^2=0$ limit and scaling by the kinematic factor $k(Q)$ in Eq. (38), as a function of Q. The contribution to the muonic hydrogen Lamb shift is proportional to the area under the curve, cf. Eq. (37).

We present in Table 3 the total structure-dependent TPE contribution to the $2P-2S$ energy splitting in muonic hydrogen. Following the terminology of Ref. [2] (cf. Table I of this reference), we write the total contribution as a sum of proton-pole, $W_1(0,Q^2)$, and continuum, contributions. Since our focus is on the impact of $W_1(0,Q^2)$, for simplicity we retain a simple dipole ansatz for the proton pole contributions.[14] The continuum contribution is from Ref. [33].

It is often conventional to subtract off a contribution to TPE corresponding to the "Sticking In Form Factors" (SIFF) ansatz [2]. With the standard dipole form factors, this contribution is[15]

$$\delta E(2P-2S)^{\text{two}-\gamma}\big|_{\text{SIFF}} = 0.0184\,\text{meV}\,. \tag{40}$$

In order to make a meaningful comparison with previous work, we add this contribution back to results where it has been subtracted.[16] The resulting total structure-dependent TPE correction from a range of approaches is displayed in Fig. 9.

[14] As in Ref. [2], we take $G_E(q^2)=G_M(q^2)/G_M(0)=[1-q^2/\Lambda^2]^{-2}$, $\Lambda^2=0.71\,\text{GeV}^2$. A more systematic evaluation of the proton pole contribution and uncertainty is considered in Ref. [32].

[15] In the literature, this may be conventionally referred to as an "elastic", "Born", or "proton" contribution.

[16] Thus we add $\delta E(2P-2S)^{\text{two}-\gamma}\big|_{\text{SIFF}}$ from Eq. (40) to the "polarizability" of Refs. [34, 35, 36, 38, 37], (for Ref. [37] we show the adjusted value quoted in Ref. [38]), and to the sum or "subtraction" and "inelastic" terms of Ref. [33]. In Refs. [3, 4] we take $\Delta E_{\text{el}}+\Delta E_{\text{np}}=0.0247\,\text{meV}\to 0.0184\,\text{meV}$. In Ref. [5], we take $\Delta E_{\text{Born}}=0.0083\,\text{meV}\to 0.0184\,\text{meV}$.

Table 3: Two-photon proton structure corrections to the $2P - 2S$ Lamb shift in muonic hydrogen, in meV.

Contribution	value (meV)
$\delta E_{\mu H}^{\rm proton}$	-0.016
$\delta E_{\mu H}^{W_1(0,Q^2)}$	0.034(13)
$\delta E_{\mu H}^{\rm continuum}$	0.0127(5)
$\delta E^{\rm two-\gamma}$	0.030(13)

5 Conclusions

The forward Compton amplitude is an important ingredient for problems in particle, nuclear and atomic physics involving nucleon structure. The subtraction function $W_1(0, Q^2)$ is a key source of uncertainty. Neither the spin-0 contribution, nor the spin-2 contribution to the leading OPE expression for this function has been correctly included previously. We computed this OPE expression and employed it to constrain the TPE contribution to the muonic-hydrogen Lamb shift.

The evaluation of $W_1(0, Q^2)$ by OPE was considered long ago by Collins [7]. This reference considered the electromagnetic corrections to the nucleon mass, where only the spin-0 contribution is relevant. As described in Sec. 3.3, an incorrect expression in Ref. [7] impacts the isoscalar spin-0 contribution. The spin-2 contribution was not considered in Ref. [7], and is found numerically to dominate the total OPE expression for $W_1^p(0, Q^2)$. For the application to the proton-neutron mass difference, both the spin-2 and the isoscalar spin-0 parts drop out.[17] However, for the application to muonic hydrogen spectroscopy these ingredients are critical.

Using a parameterization of higher order corrections, Eqs. (34) and (36), an interpolation of $W_1(0, Q^2)$ with the correct low-Q^2 and high-Q^2 behavior is displayed in Fig. 7. The corresponding TPE contribution and uncertainty for the Lamb shift in muonic hydrogen is given by the area under the curve in Fig. 8, as displayed in Fig. 9. This uncertainty remains the dominant one in the muonic hydrogen Lamb shift, and for derived observables such as the proton charge radius and Rydberg constant using muonic hydrogen inputs. Further constraints arising from chiral lagrangian analysis in the $m_\pi^2 \lesssim Q^2 \ll m_p^2$ regime are discussed in Appendix B. Obtaining an error bar of the size assumed in the CREMA analysis [31] (the point corresponding to Ref. [4] in Fig. 9) requires some level of model dependence. Future measurements with light muonic atoms and questions surrounding the proton radius puzzle may motivate direct computations using lattice QCD.

Acknowledgments

We thank J. Arrington, A. Blechman, G. Lee, A. Majumder, A. Walker-Loud, I. Yavin and

[17] These observations imply that the electromagnetic contribution to the neutron-proton mass difference cannot be used to directly constrain the TPE contribution to muonic hydrogen spectroscopy.

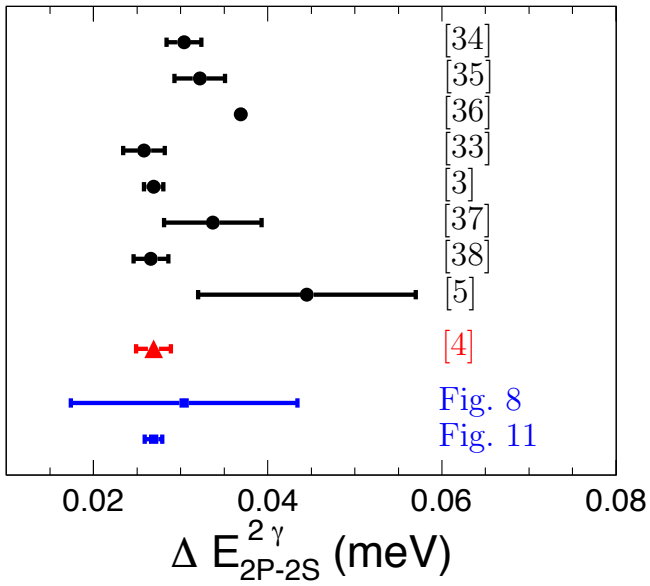

Figure 9: Two-photon contribution to the Lamb shift in muonic hydrogen, adjusted to common proton elastic form factors (see text). Black circles denote previous work, blue square denotes the present work. The red triangle is the summary of Ref. [4] used in the CREMA muonic hydrogen extraction of r_E^p.

Z. Ye for useful discussions. G.P. thanks Perimeter Institute for Theoretical Physics, where part of this work was done, for its hospitality and support. This work was supported by NIST Precision Measurement Grants Program (R.J.H., G.P.), DOE grant DE-FG02-13ER41958 (R.J.H.) and DOE grant DE-SC0007983 (G.P.). Research at Perimeter Institute is supported by the Government of Canada through the Department of Innovation, Science and Economic Development and by the Province of Ontario through the Ministry of Research and Innovation. TRIUMF receives federal funding via a contribution agreement with the National Research Council of Canada. Fermilab is operated by Fermi Research Alliance, LLC under Contract No. DE-AC02-07CH11359 with the United States Department of Energy.

A Details on gluon operator structures

In the calculation we encounter the structure $q_\alpha q_\beta G^{A\mu\alpha} G^{A\nu\beta}$. $G^{A\mu\alpha} G^{A\nu\beta}$ is the color-singlet product of a chromo-electric (E_i^A) and a chromo-magnetic (B_i^A) field. As such, it has $7\times 6/2 = 21$ linearly independent components. Since $q_\alpha q_\beta G^{A\mu\alpha} G^{A\nu\beta}$ depends only on the symmetric part of $G^{A\mu\alpha} G^{A\nu\beta}$ under $\alpha \leftrightarrow \beta$, it can be written in terms of the four-index tensor $O_{\rm S}^{\mu\alpha\nu\beta} \equiv \frac{1}{2}\left(G^{A\mu\alpha} G^{A\nu\beta} + G^{A\mu\beta} G^{A\nu\alpha}\right)$ as $q_\alpha q_\beta O_{\rm S}^{\mu\alpha\nu\beta}$. The tensor $O_{\rm S}^{\mu\alpha\nu\beta}$ has the index symmetries $O_{\rm S}^{\mu\alpha\nu\beta} = O_{\rm S}^{\mu\beta\nu\alpha} = O_{\rm S}^{\nu\beta\mu\alpha}$ and 20 linearly independent components. Nine of these can be identified with the components of $O_g^{(2)\alpha\beta}$ and one with $O_g^{(0)}$.

Following [14], define

$$O^{(0)\mu\alpha\nu\beta} = \frac{1}{d(d-1)} O_g^{(0)} \left(g^{\mu\nu}g^{\alpha\beta} - g^{\mu\beta}g^{\nu\alpha}\right) ,$$

$$O^{(2)\mu\alpha\nu\beta} = \frac{1}{d-2} \left(g^{\mu\beta}O_g^{(2)\nu\alpha} + g^{\nu\alpha}O_g^{(2)\mu\beta} - g^{\mu\nu}O_g^{(2)\alpha\beta} - g^{\alpha\beta}O_g^{(2)\mu\nu}\right) , \tag{41}$$

and $O_{\rm S}^{(0)\mu\alpha\nu\beta} = \frac{1}{2}\left(O^{(0)\mu\alpha\nu\beta} + O^{(0)\mu\beta\nu\alpha}\right)$, $O_{\rm S}^{(2)\mu\alpha\nu\beta} = \frac{1}{2}\left(O^{(2)\mu\alpha\nu\beta} + O^{(2)\mu\beta\nu\alpha}\right)$. We can write $O_{\rm S}^{\mu\alpha\nu\beta}$ as

$$O_{\rm S}^{\mu\alpha\nu\beta} = O_{\rm S}^{(0)\mu\alpha\nu\beta} + O_{\rm S}^{(2)\mu\alpha\nu\beta} + O_{\rm S}^{(r)\mu\alpha\nu\beta}. \tag{42}$$

The last term $O_{\rm S}^{(r)\mu\alpha\nu\beta}$ can be expressed explicitly as

$$O_{\rm S}^{(r)\mu\alpha\nu\beta} = -\frac{1}{4}\left(\epsilon^{\mu\alpha\rho\sigma}\epsilon^{\nu\beta\kappa\lambda} + \epsilon^{\mu\beta\rho\sigma}\epsilon^{\nu\alpha\kappa\lambda}\right) G^A_{\rho\kappa}G^A_{\sigma\lambda} - \text{all possible traces.} \tag{43}$$

Since a product of two Levi-Civita tensors can be expressed in terms of the metric tensor, Eq. (43) can be shown to be equivalent to Eq. (42).

The matrix elements of $O_S^{\mu\alpha\nu\beta}$ between spin-averaged proton states can be expressed in terms of the matrix elements of $G^{A\mu\alpha}G^{A\nu\beta}$. These can depend only on the metric tensor and powers of the proton four-momentum, k. We can have six structures $g^{\mu\nu}g^{\alpha\beta}$, $g^{\mu\beta}g^{\nu\alpha}$, $g^{\mu\nu}k^\alpha k^\beta$, $g^{\alpha\beta}k^\mu k^\nu$, $g^{\mu\beta}k^\nu k^\alpha$, and $g^{\nu\alpha}k^\mu k^\beta$ with arbitrary coefficients.[18] The matrix elements of $G^{A\mu\alpha}G^{A\nu\beta}$ are antisymmetric under $\mu \leftrightarrow \alpha$ and $\nu \leftrightarrow \beta$. As a result, only two of the six coefficients are independent. These can be identified with the matrix elements of the spin-0 and spin-2 gluonic operators. In particular this implies that the matrix elements of $O_{\rm S}^{(r)\mu\alpha\nu\beta}$ between spin-averaged proton states vanish. Working in d-dimensions we find the useful operator relation,

$$\frac{q_\alpha q_\beta}{q^2} G^{A\mu\alpha}G^{A\nu\beta} = -\frac{1}{d(d-1)} O_g^{(0)} \left(-g^{\mu\nu} + \frac{q^\mu q^\nu}{q^2}\right) + \frac{q_\alpha q_\beta}{q^2} O^{(2)\mu\alpha\nu\beta} + \frac{q_\alpha q_\beta}{q^2} O_{\rm S}^{(r)\mu\alpha\nu\beta}, \tag{44}$$

from which we obtain the expression for $T_c^{\mu\nu}$.

B Chiral lagrangian constraints

Let us consider potential improvements to the low-Q^2 constraints on the interpolation displayed in Fig. 7. Recall that the results (33) are obtained by a straightforward computation from the NRQED lagrangian. The relevant NRQED Wilson coefficients are determined by Taylor expansions of conventionally-defined relativistic form factors and Compton scattering amplitudes. In principle, a similar strategy can be applied at higher orders in the low-Q^2 expansion. However, the NRQED lagrangian is not available through the relevant $(1/M^5)$ order, nor has the scattering data yet been analyzed with this application in mind.

[18] The structure $k^\mu k^\nu k^\alpha k^\beta$ is symmetric in $\mu \leftrightarrow \alpha$ and $\nu \leftrightarrow \beta$.

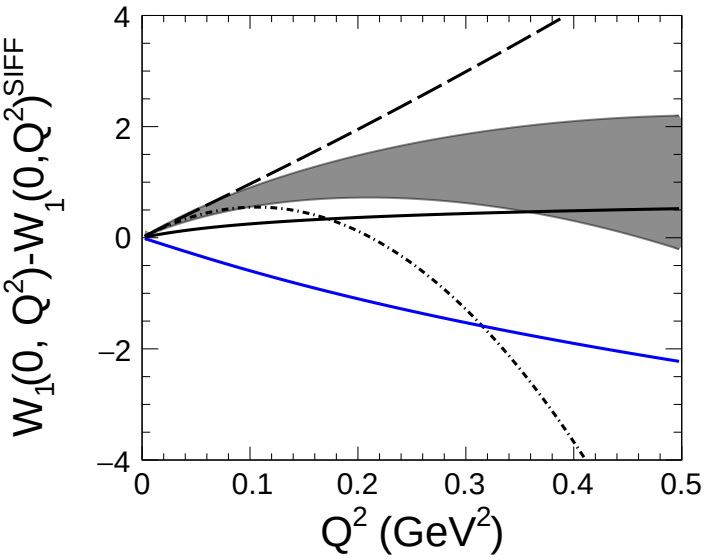

Figure 10: Different calculations of $W_1(0,Q^2) - W_1(0,Q^2)^{\rm SIFF}$. The black solid line, black dashed line, and solid band, give the "third-order" ($\overline{T}_1^{(3)}$), "fourth-order" ($\overline{T}_1^{(3)} + \overline{T}_1^{(4)}$), and "fourth-order plus Δ" ($\overline{T}_1^{(3)} + \overline{T}_1^{(4)} + \overline{T}_1^{(\Delta)}$) results of Ref. [3], using the parameters of Ref. [3] and their prescription for determining $\delta\beta$. The solid band adds in quadrature the errors from c_1, c_2, c_3, β and $g_{\pi {\rm N}\Delta}$. The dash-dotted black line gives the fourth order plus Δ contribution ($\overline{T}_1^{(3)} + \overline{T}_1^{(4)} + \overline{T}_1^{(\Delta)}$), Taylor expanded through $\mathcal{O}(Q^4)$. The bottom blue solid line gives the "third order" ($T_1^{({\rm NB})}(0,Q^2)$) result of Ref. [38], using its parameters.

Chiral lagrangian analysis can in principle be used to further constrain $W_1(0,Q^2)$ in the regime where a finite number of hadronic excitations are relevant.[19] As usual, the error budget should account for scheme choices, such as whether $n_f = 2$ or $n_f = 3$ light flavors are considered, whether formally higher-order terms are included at each order in the expansion, and how Δ excitations are treated. Fig. 10 shows the low-Q^2 behavior of $W_1(0,Q^2) - W_1(0,Q^2)^{\rm SIFF}$ in several calculational schemes, where $W_1(0,Q^2)^{\rm SIFF}$ denotes a conventional subtraction term involving elastic form factors.[20] Let us consider at face value the error budget from Ref. [3] to constrain the deviation from $W_1(0,Q^2)^{\rm SIFF}$ below $Q^2 = (500\,{\rm MeV})^2$. Neglecting the uncertainty on the SIFF contribution,[21] the corresponding interpolation is displayed in Fig. 11. Also displayed in Fig. 11 are upper and lower envelopes corresponding to alternative schemes

[19] We remark that this is a distinct application of chiral lagrangian analysis compared to the two-step matching of QCD onto NRQED with chiral lagrangian as intermediate theory [5]. We are here directly matching QCD onto NRQED, using experimental data supplemented with constraints on $W_1(0,Q^2)$ to determine the forward Compton amplitude as the relevant hadronic input.

[20] A transcription error appears in Ref. [3]: the second term in (A.4) should have the opposite sign [39].

[21] Form factor curvature and higher-order terms in the Taylor expansion of form factors are poorly constrained by data, but the existence of data-driven constraints on $F_i(q^2)$ throughout the relevant range of q^2 should drive a relatively small uncertainty for this contribution.

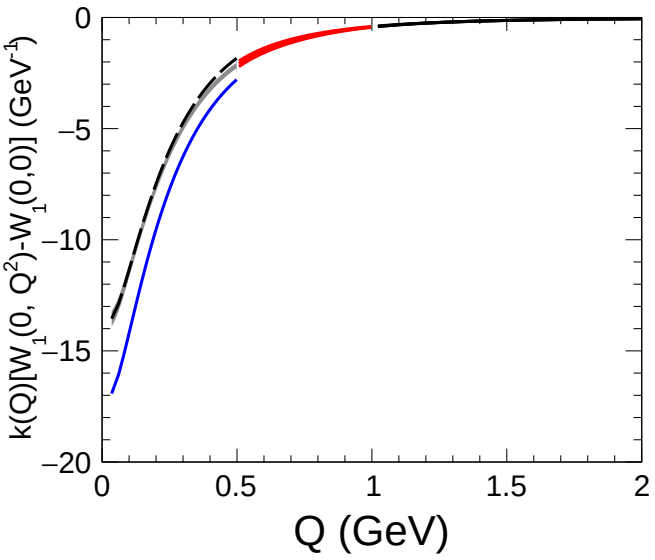

Figure 11: Same as Fig. 8, but with $W_1(0,Q^2)$ at low-Q^2 taken as $W_1(0,Q^2)^{\rm SIFF}$ with dipole nucleon form factors, and deviation from $W_1(0,Q^2)^{\rm SIFF}$ given by the band in Fig. 10.

displayed in Fig. 10.

Whether it is possible to compute the difference $W_1(0,Q^2) - W_1(0,Q^2)^{\rm SIFF}$ more precisely than $W_1(0,Q^2)$ itself, and how best to assign an error budget that accounts for computational scheme dependence in Fig. 10, remain difficult questions. Figure 11 illustrates the potential to combine low-Q^2 constraints with the OPE.

References

[1] R. Pohl *et al.*, Nature **466**, 213 (2010).

[2] R. J. Hill and G. Paz, Phys. Rev. Lett. **107**, 160402 (2011).

[3] M. C. Birse and J. A. McGovern, Eur. Phys. J. A **48**, 120 (2012).

[4] A. Antognini, F. Kottmann, F. Biraben, P. Indelicato, F. Nez and R. Pohl, Annals Phys. **331**, 127 (2013).

[5] C. Peset and A. Pineda, Nucl. Phys. B **887**, 69 (2014).

[6] W. N. Cottingham, Annals Phys. **25**, 424 (1963).

[7] J. C. Collins, Nucl. Phys. B **149**, 90 (1979) Erratum: [Nucl. Phys. B **153**, 546 (1979)].

[8] A. Walker-Loud, C. E. Carlson and G. A. Miller, Phys. Rev. Lett. **108**, 232301 (2012).

[9] F. B. Erben, P. E. Shanahan, A. W. Thomas and R. D. Young, Phys. Rev. C **90**, no. 6, 065205 (2014).

[10] J. Gasser, M. Hoferichter, H. Leutwyler and A. Rusetsky, Eur. Phys. J. C **75**, no. 8, 375 (2015).

[11] W. E. Caswell and G. P. Lepage, Phys. Lett. **167B**, 437 (1986).

[12] R. J. Hill, G. Lee, G. Paz and M. P. Solon, Phys. Rev. D **87**, 053017 (2013).

[13] V. A. Novikov, M. A. Shifman, A. I. Vainshtein and V. I. Zakharov, Fortsch. Phys. **32**, 585 (1984).

[14] R. J. Hill and M. P. Solon, Phys. Rev. D **91**, 043504 (2015).

[15] R. J. Hill and M. P. Solon, Phys. Rev. D **91**, 043505 (2015).

[16] S. Durr *et al.*, Phys. Rev. D **85**, 014509 (2012) Erratum: [Phys. Rev. D **93**, no. 3, 039905 (2016)].

[17] S. Durr *et al.*, Phys. Rev. Lett. **116**, no. 17, 172001 (2016).

[18] Y. B. Yang *et al.* [xQCD Collaboration], Phys. Rev. D **94**, no. 5, 054503 (2016).

[19] A. Abdel-Rehim *et al.* [ETM Collaboration], Phys. Rev. Lett. **116**, no. 25, 252001 (2016).

[20] G. S. Bali *et al.* [RQCD Collaboration], Phys. Rev. D **93**, no. 9, 094504 (2016).

[21] M. Hoferichter, J. Ruiz de Elvira, B. Kubis and U. G. Meiner, Phys. Rev. Lett. **115**, 092301 (2015).

[22] J. Gasser and H. Leutwyler, Phys. Rept. **87**, 77 (1982).

[23] A. Crivellin, M. Hoferichter and M. Procura, Phys. Rev. D **89**, 054021 (2014).

[24] C. Patrignani *et al.* [Particle Data Group Collaboration], Chin. Phys. C **40**, no. 10, 100001 (2016).

[25] P. Junnarkar and A. Walker-Loud, Phys. Rev. D **87**, 114510 (2013).

[26] W. Freeman *et al.* [MILC Collaboration], Phys. Rev. D **88**, 054503 (2013).

[27] M. Gong *et al.* [XQCD Collaboration], Phys. Rev. D **88**, 014503 (2013).

[28] A. D. Martin, W. J. Stirling, R. S. Thorne and G. Watt, Eur. Phys. J. C **63**, 189 (2009).

[29] G. Lee, J. R. Arrington and R. J. Hill, Phys. Rev. D **92**, no. 1, 013013 (2015).

[30] P. J. Mohr, D. B. Newell and B. N. Taylor, Rev. Mod. Phys. **88**, no. 3, 035009 (2016).

[31] A. Antognini *et al.*, Science **339**, 417 (2013).

[32] J. R. Arrington, R. J. Hill, G. Lee and Z. Ye, *in preparation.*

[33] C. E. Carlson and M. Vanderhaeghen, Phys. Rev. A **84**, 020102 (2011).

[34] K. Pachucki, Phys. Rev. A **60**, 3593 (1999).

[35] A. P. Martynenko, Phys. Atom. Nucl. **69**, 1309 (2006).

[36] D. Nevado and A. Pineda, Phys. Rev. C **77**, 035202 (2008).

[37] M. Gorchtein, F. J. Llanes-Estrada and A. P. Szczepaniak, Phys. Rev. A **87**, no. 5, 052501 (2013).

[38] J. M. Alarcon, V. Lensky and V. Pascalutsa, Eur. Phys. J. C **74**, no. 4, 2852 (2014).

[39] M. C. Birse and J. A. McGovern, private communication.